DALTON
FULL PAPER

Two new one-dimensional systems with end-to-end single dicyanamide bridges between manganese(II) centres: structural and magnetic properties

Albert Claramunt,[a] **Albert Escuer,**[a] **Franz A. Mautner,**[b] **Núria Sanz**[a] **and Ramon Vicente** *[a]

[a] *Departament de Química Inorgànica, Universitat de Barcelona, Diagonal 647, 08028 Barcelona, Spain. E-mail: rvicente@kripto.qui.ub.es*

[b] *Institut für Physikalische und Theoretische Chemie, Technische Universität Graz, A-8010 Graz, Austria*

Received 20th March 2000, Accepted 13th June 2000
Published on the Web 13th July 2000

Dicyanamide, $[N(CN)_2]^-$ (dca), formed monodimensional compounds of formula $[Mn(\mu_{1,5}\text{-dca})(NO_3)(terpy)]_n$ **1** and $[Mn(\mu_{1,5}\text{-dca})(H_2O)(terpy)]_n[dca]_n$ **2** (terpy = 2,2′:6′,2″-terpyridine). X-Ray diffraction analysis revealed two one-dimensional systems with single dca bridges. The manganese atom in **1** is seven-co-ordinated, with a MnN_5O_2 pentagonal bipyramidal environment, whereas in **2** the manganese atom is six-co-ordinated. Susceptibility measurements of **1** and **2** indicate slight antiferromagnetic coupling.

Introduction

Dicyanamide (dca) bridged polynuclear systems are a fast growing research field due to the large variety of topologies and magnetic properties that may be obtained from this ligand. Dicyanamide may act potentially as a bidentate ligand by co-ordination to two different metallic centres by means of the terminal N(nitrile) atoms, or as a tridentate ligand by means of the additional co-ordination of the central N(amide) atom. Tridentate co-ordination has been obtained in several neutral 3-D compounds of general formula $[M(dca)_2]$ (M^{II} = Fe, Mn, Co, Ni or Cu), showing a rutile-like structure.[1–4] Lower dimensional systems with general formula $[M(L)_2(dca)_2]$, L = unidentate ligand, have also been obtained by co-ordination of two blocking L ligands. In this case the four remaining co-ordination sites are occupied by the N(nitrile) atoms of the dca ligands, leading to square two-dimensional systems with each metal centre bridged by means of four single end-to-end dca to four neighbouring ones[5–7] or one-dimensional systems with double end-to-end dca bridges along the chains.[8–11] Magnetic interactions reported to date are generally low, but the different kind of interactions reported for Co^{II} and Ni^{II} (ferromagnetic) or Fe^{II} and Mn^{II} (antiferromagnetic) are still unclear and deserve attention of magnetochemists. The topologies of $[M(L)_2(\mu_{1,5}\text{-dca})_2]$ are closely related with some similar 2-D or 1-D $[M(L)_2(\mu_{1,3}\text{-}N_3)_2]$ compounds and several authors have explored both kinds of bridging ligands.[10–13]

Following our work in this field we report the synthesis and magneto-structural characterisation of two new one-dimensional dca derivatives with formula $[Mn(\mu_{1,5}\text{-dca})(NO_3)(terpy)]_n$ **1** and $[Mn(\mu_{1,5}\text{-dca})(H_2O)(terpy)]_n[dca]_n$ **2** (terpy = 2,2′:6′,2″-terpyridine) and single dca bridges. In these compounds the dca co-ordination mode is end-to-end, by means of the N(nitrile) atoms, and the use of the tridentate terpy ligand helps stabilise the one-dimensional system.

Experimental

Synthesis

$[Mn(\mu_{1,5}\text{-dca})(NO_3)(terpy)]_n$ was synthesized by adding 0.4 mmol of 2,2′:6′,2″-terpyridine to a solution of 0.4 mmol of manganese(II) nitrate hexahydrate in 25 ml of methanol, followed by dropwise addition of 0.8 mmol of sodium dicyanamide in the minimum of water. After filtering from a little precipitate, the clear solution was left to stand in the air for several days. In four days, pale yellow crystals suitable for X-ray determination were formed. Yield 48%. Found (calc.) for $C_{17}H_{11}MnN_7O_3$: C, 49.5 (49.0); H, 2.8 (2.7); N, 23.9 (23.5).

$[Mn(\mu_{1,5}\text{-dca})(H_2O)(terpy)]_n[dca]_n$ was synthesized by adding 1 mmol of 2,2′:6′,2″-terpyridine to a solution of 1 mmol of manganese(II) triflate tetrahydrate in 30 ml of methanol, followed by dropwise addition of 2.0 mmol of sodium dicyanamide in the minimum of water. The clear solution was left to stand in the air for several days. In two days, pale yellow crystals suitable for X-ray determination were formed. Yield 55%. Found (calc.) for $C_{19}H_{13}MnN_9O$: C, 52.9 (52.1); H, 3.2 (3.0); N, 28.2 (28.7).

Physical measurements

Spectral and magnetic. Magnetic susceptibility measurements were carried out for compound **1** on polycrystalline samples with a SQUID apparatus working in the range 2–300 K under a magnetic field of 0.05 T. Magnetic measurements were carried out for **2** with a Faraday type magnetometer (MANICS DSM8) equipped with an Oxford CF 1200 S helium continuous-flow cryostat working in the temperature range 300–4 K under a magnetic field of 1.5 T. Diamagnetic corrections were estimated from Pascal Tables. EPR spectra were recorded with a Bruker ES200 spectrometer at X-band frequency.

Crystal structure determination. X-Ray single-crystal data for $[Mn(\mu_{1,5}\text{-dca})(NO_3)(terpy)]_n$ **1** and $[Mn(\mu_{1,5}\text{-dca})(H_2O)(terpy)]_n[dca]_n$ **2** were collected on a modified STOE four-circle diffractometer. The crystallographic data, conditions for the intensity data collection, and some features of the structure refinement are listed in Table 1. Additional corrections for intensity decay were applied for data processing. The structures were solved by direct methods using the SHELXS 86[14] computer program, and refined by full-matrix least-squares methods on F^2 using SHELXL 93[15] incorporated in the SHELXTL/PC V 5.03[16] program library and the graphics program PLUTON.[17] All non-hydrogen atoms were refined anisotropically and the hydrogen atoms fixed geometrically with the HFIX utility.[16]

CCDC reference number 186/2031.

DOI: 10.1039/b002214o

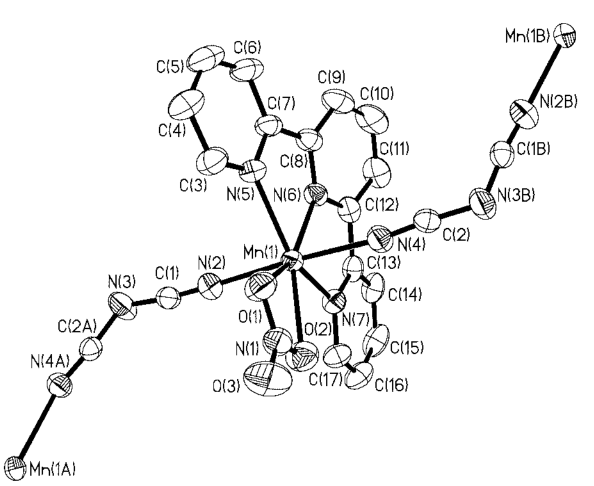

Fig. 1 An ORTEP plot (40% probability ellipsoids) and atom labelling scheme of [Mn($\mu_{1,5}$-dca)(NO_3)(terpy)]$_n$ **1**, with pentagonal bipyramidal Mn^{II}.

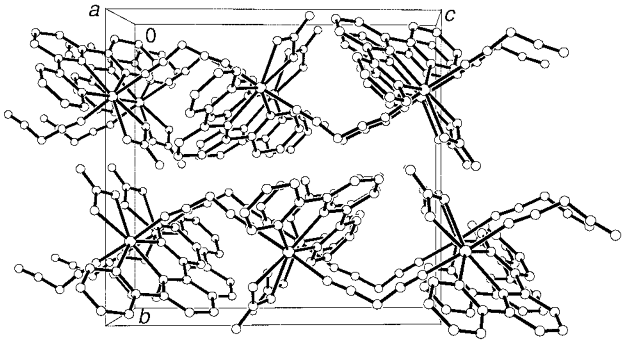

Fig. 2 Cell plot of [Mn($\mu_{1,5}$-dca)(NO_3)(terpy)]$_n$ **1**: the chains of polyhedra are oriented along [1 0 1].

See http://www.rsc.org/suppdata/dt/b0/b002214o/ for crystallographic files in .cif format.

Results and discussion

Crystal structures

***trans*-[Mn($\mu_{1,5}$-dca)(NO_3)(terpy)]$_n$ 1.** A labelled ORTEP[18] plot of the structure of *trans*-[Mn($\mu_{1,5}$-dca)(NO_3)(terpy)]$_n$ is shown in Fig. 1. The structure of the compound consists of well isolated chains of manganese atoms bridged by means of single end-to-end dicyanamide bridges (Fig. 2). Each manganese atom is seven-co-ordinated, with a co-ordination polyhedron close to a pentagonal bipyramid, by means of three N atoms belonging to the terpyridine ligand and two oxygen atoms from the bidentate nitrato ligand, which determines the equatorial plane, and finally two N atoms in *trans* disposition from the bridging dicyanamide ligands. The shorter bond lengths, 2.196(3) Å and 2.218(3) Å (Table 2), correspond to the axial position occupied by the dca ligand, Mn(1)–N(2) and Mn(1)–N(4) respectively, whereas the equatorial sites show similar bond lengths in the 2.271–2.318 Å range, with the exception of the Mn(1)–O(2) bond (2.390(3) Å). Three kinds of bond angles may be found in the equatorial plane: the lower of 53.91(11)° corresponds to the bidentate nitrato ligand O(1)–Mn(1)–O(2) bond angle, two intermediate ones of 70.1(1) and 71.0(1)° corresponding to the N(terpy)–Mn(1)–N(terpy) bond angles and two greater O(nitrato)–Mn(1)–N(terpy) bond angles of 81.5(1) and 84.3(1)°. The five equatorial donor atoms and the central manganese atom determine a plane with maximum deviation for N(6) of −0.196(3) Å, whereas the remaining atoms show deviations lower than 0.130 Å. Planarity of this unit may also be envisaged by the sum of the neighbouring bond angles of 360.8°. The terpyridine ligand is not fully planar, the average angles between the three different rings being 15.5°. Bond angles related to the dicyanamide ligands, which occupies the axial positions of the pentagonal bipyramid, are 177.5(3) and 166.3(3)° for Mn(1)–N(2)–C(1) and Mn(1)–N(4)–C(2) respectively. The central C(1)–N(3)–C(2A) angle is 120.4(4)°. The shorter Mn · · · Mn intrachain distance is 8.147(3) Å, in the same range as the shortest Mn · · · Mn interchain distances of 8.033(3), 8.255(3) and 8.331(3) Å.

Table 1 Crystal data and structure refinement for [Mn($\mu_{1,5}$-dca)(NO_3)(terpy)]$_n$ **1** and [Mn($\mu_{1,5}$-dca)(H_2O)(terpy)]$_n$[dca]$_n$ **2**

	1	**2**
Formula	$C_{17}H_{11}MnN_7O_3$	$C_{19}H_{13}MnN_9O$
Formula weight	416.27	438.32
Crystal system	Monoclinic	Triclinic
Space group	$P2_1/n$ (no. 14)	$P\bar{1}$ (no. 2)
a/Å	8.825(3)	7.574(2)
b/Å	13.928(4)	8.795(3)
c/Å	14.650(4)	14.948(6)
α/°		78.16(3)
β/°	96.05(3)	79.73(3)
γ/°		81.80(2)
V/Å^3	1790.7(9)	953.1(6)
Z	4	2
T/°C	25(2)	27(2)
λ(Mo-Kα)/Å	0.71069	0.71069
μ(Mo-Kα)/mm^{-1}	0.772	0.725
R	0.0553	0.0372
$wR2$	0.1436	0.0947

Table 2 Selected bond lengths (Å) and angles (°) for [Mn($\mu_{1,5}$-dca)(NO_3)(terpy)]$_n$ **1**

Mn(1)–N(2)	2.196(3)	Mn(1)–N(4)	2.218(3)
Mn(1)–N(6)	2.271(3)	Mn(1)–O(1)	2.289(3)
Mn(1)–N(7)	2.291(3)	Mn(1)–N(5)	2.318(3)
Mn(1)–O(2)	2.390(3)	N(1)–O(3)	1.203(5)
N(1)–O(1)	1.253(4)	N(1)–O(2)	1.257(5)
N(2)–C(1)	1.134(5)	C(1)–N(3)	1.300(5)
N(3)–C(2a)	1.302(5)	C(2)–N(4)	1.141(4)
C(2)–N(3b)	1.302(5)		
N(2)–Mn(1)–N(4)	176.31(13)	N(2)–Mn(1)–N(6)	99.71(12)
N(4)–Mn(1)–N(6)	83.51(12)	N(2)–Mn(1)–O(1)	90.78(13)
N(4)–Mn(1)–O(1)	87.26(12)	N(6)–Mn(1)–O(1)	149.57(11)
N(2)–Mn(1)–N(7)	88.77(13)	N(4)–Mn(1)–N(7)	90.60(12)
N(6)–Mn(1)–N(7)	70.96(11)	O(1)–Mn(1)–N(7)	138.25(11)
N(2)–Mn(1)–N(5)	90.11(12)	N(4)–Mn(1)–N(5)	92.70(12)
N(6)–Mn(1)–N(5)	70.08(12)	O(1)–Mn(1)–N(5)	81.51(11)
N(7)–Mn(1)–N(5)	140.23(12)	N(2)–Mn(1)–O(2)	89.55(13)
N(4)–Mn(1)–O(2)	86.76(12)	N(6)–Mn(1)–O(2)	153.27(12)
O(1)–Mn(1)–O(2)	53.91(11)	N(7)–Mn(1)–O(2)	84.34(11)
N(5)–Mn(1)–O(2)	135.41(12)	O(3)–N(1)–O(1)	121.6(4)
O(3)–N(1)–O(2)	122.8(4)	O(1)–N(1)–O(2)	115.5(3)
N(1)–O(1)–Mn(1)	97.8(2)	N(1)–O(2)–Mn(1)	92.8(2)
C(1)–N(2)–Mn(1)	177.5(3)	N(2)–C(1)–N(3)	173.3(4)
C(2a)–N(3)–C(1)	120.4(4)	N(4)–C(2)–N(3b)	174.5(4)
C(2)–N(4)–Mn(1)	166.3(3)		

Symmetry codes: a $x + \frac{1}{2}, -y + \frac{1}{2}, z + \frac{1}{2}$; b $x - \frac{1}{2}, -y + \frac{1}{2}, z - \frac{1}{2}$.

***cis*-[Mn($\mu_{1,5}$-dca)(H_2O)(terpy)]$_n$[dca]$_n$ 2.** A labelled ORTEP plot of the structure of *cis*-[Mn($\mu_{1,5}$-dca)(H_2O)(terpy)]$_n$[dca]$_n$ is shown in Fig. 3. The compound consists of two kinds of chains: *cis* chains of manganese atoms bridged by means of two single end-to-end dicyanamide bridges and, perpendicularly, chains built from non-co-ordinated dicyanamide anions and co-ordinated water molecules bridged by hydrogen bonds (Fig. 4). Each manganese atom is six-co-ordinated: three N atoms belonging to the terpyridine ligand and one N atom of one bridging dicyanamide ligand are in the same plane. Perpendicular to this plane are placed the oxygen atom of the co-ordinated water molecule and the N atom of the other bridging dicyanamide ligand. The shorter bond lengths, 2.162(2) and

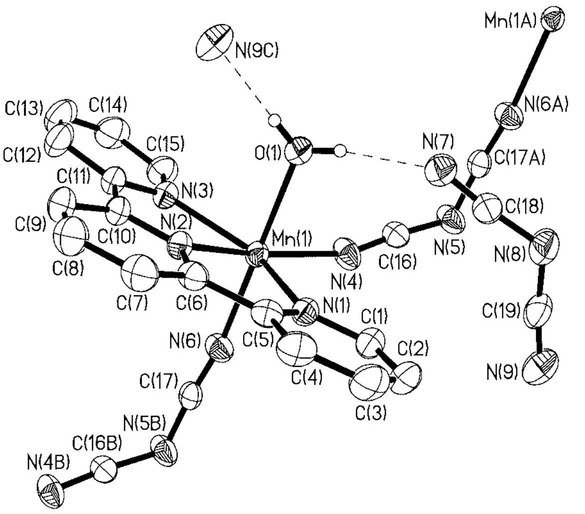

Fig. 3 An ORTEP plot (40% probability ellipsoids) and atom labelling scheme of $[Mn(\mu_{1,5}\text{-dca})(H_2O)(terpy)]_n[dca]_n$ **2**.

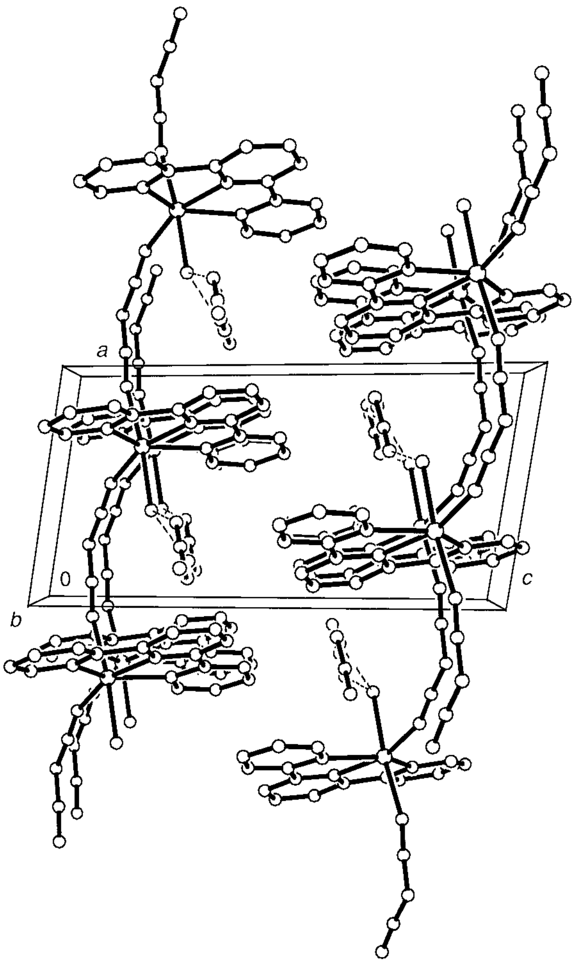

Fig. 4 Packing of $[Mn(\mu_{1,5}\text{-dca})(H_2O)(terpy)]_n[dca]_n$ **2**, along the *b* axis of the unit cell.

Table 3 Selected bond lengths (Å) and angles (°) for $[Mn(\mu_{1,5}\text{-dca})(H_2O)(terpy)]_n[dca]_n$ **2**

Mn(1)–N(4)	2.162(2)	Mn(1)–N(6)	2.182(2)
Mn(1)–N(2)	2.233(2)	Mn(1)–O(1)	2.230(2)
Mn(1)–N(3)	2.288(2)	Mn(1)–N(1)	2.287(2)
N(4)–C(16)	1.145(3)	C(16)–N(5)	1.297(3)
N(5)–C(17a)	1.294(3)	C(17)–N(6)	1.145(3)
C(17)–N(5b)	1.294(3)	N(7)–C(18)	1.144(3)
C(18)–N(8)	1.299(3)	N(8)–C(19)	1.298(3)
C(19)–N(9)	1.140(3)		
N(4)–Mn(1)–N(6)	95.05(7)	N(4)–Mn(1)–N(2)	162.08(7)
N(6)–Mn(1)–N(2)	97.80(7)	N(4)–Mn(1)–O(1)	81.41(7)
N(6)–Mn(1)–O(1)	174.23(7)	N(2)–Mn(1)–O(1)	86.67(7)
N(4)–Mn(1)–N(3)	120.14(8)	N(6)–Mn(1)–N(3)	92.40(7)
N(2)–Mn(1)–N(3)	71.81(7)	O(1)–Mn(1)–N(3)	85.51(7)
N(4)–Mn(1)–N(1)	95.82(8)	N(6)–Mn(1)–N(1)	92.64(7)
N(2)–Mn(1)–N(1)	71.22(7)	O(1)–Mn(1)–N(1)	92.25(7)
N(3)–Mn(1)–N(1)	143.03(7)	N(4)–C(16)–N(5)	174.0(2)
C(17a)–N(5)–C(16)	121.9(2)	N(6)–C(17)–N(5b)	173.6(2)
C(17)–N(6)–Mn(1)	164.0(2)	N(7)–C(18)–N(8)	173.8(3)
C(19)–N(8)–C(18)	120.5(2)	N(9)–C(19)–N(8)	172.4(3)
Hydrogen bonds			
O(1) · · · N(7)	2.831(3)	O(1) · · · N(9c)	2.795(3)
O(1)–H(5)	0.85(2)	O(1)–H(6)	0.83(2)
H(5) · · · N(7)	2.00(2)	H(6) · · · N(9c)	1.97(2)
N(7) · · · O(1) · · · N(9c)	118.14(9)	H(5)–O(1)–H(6)	110(3)
O(1)–H(5) · · · N(7)	169(3)	O(1)–H(6) · · · N(9c)	177(3)

Symmetry codes: a $x + 1, y, z$; b $x - 1, y, z$; c $x, y - 1, z$.

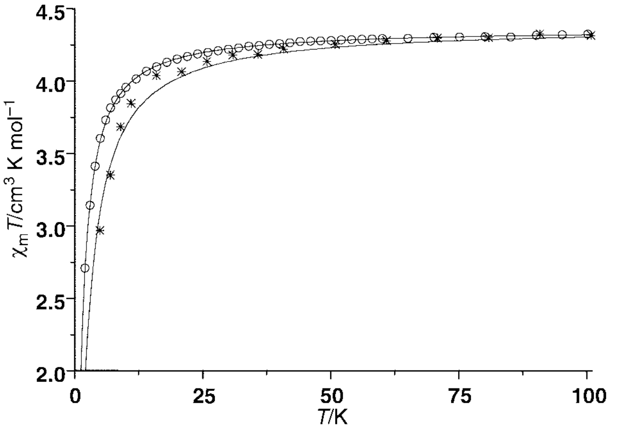

Fig. 5 Plot of the $\chi_m T$ product *vs.* *T* for compounds $[Mn(\mu_{1,5}\text{-dca})(NO_3)(terpy)]_n$ **1** (circles) and $[Mn(\mu_{1,5}\text{-dca})(H_2O)(terpy)]_n[dca]_n$ **2** (asterisks); the solid lines show the best fit theoretical curves (see text).

2.182(2) Å (Table 3), correspond to the Mn–N(dca) distances, Mn(1)–N(4) and Mn(1)–N(6) respectively, whereas the Mn–N(terpy) bond lengths are in the 2.233–2.288 Å range. The Mn(1)–O(1) bond length is 2.230(2) Å. Owing to the structural rigidity of the terpyridine ligand, the bond angles in the Mn–terpy–N(4) plane are far off the expected for an ideal octahedral geometry: N(2)–Mn(1)–N(3), N(2)–Mn(1)–N(1), N(4)–Mn(1)–N(1) and N(4)–Mn(1)–N(3) are 71.81(7), 71.22(7), 95.82(8) and 120.14(8)° respectively. The chemically equivalent bond angles N(4)–Mn(1)–N(1) and N(4)–Mn(1)–N(3) are significantly different as a consequence of packing (Fig. 4). As in **1**, the terpyridine ligand is not fully planar: the acute angles between terpy ring planes are: rings N(1)–C(5) and N(2)–C(10), 3.4(1)°; rings N(2)–C(10) and N(3)–C(15), 6.1(1)°. The bond angles related to the bridging dicyanamide ligand are Mn(1)–N(6)–C(17), Mn(1)–N(4)–C(16) and C(17a)–N(5)–C(16): 164.0(2), 155.6(2) and 121.9(2)° respectively. The structural parameters for the anionic dicyanamide are similar to the same parameters for the bridging dicyanamide ligand (see Table 3). The shorter Mn · · · Mn intrachain distance is 7.574(3) Å, in the same range as the shortest Mn · · · Mn interchain distances of 7.073(3), 7.165(3) and 8.265(4) Å.

Magnetic properties

The $\chi_m T$ product *vs.* *T* in the 100–4 K range for compounds **1** and **2** is plotted in Fig. 5. The overall behaviour corresponds to antiferromagnetically coupled systems: $\chi_m T$ decreases on cooling from 4.3 cm^3 K mol^{-1} at 100 K and tends to zero at low temperature, whereas the χ_m *vs.* *T* plot increases on cooling and has no maximum in the temperature range studied. The magnetic data of **1** and **2**, according to an homogeneous chain structure, were analysed by means of the analytical expression[19] derived by Fisher for the magnetic susceptibility of an infinite chain of classical spins based on the Hamiltonian $H = -J\Sigma S_iS_{i+1}$ for local spin values $S = 5/2$. The best fit parameters were: $J = -0.12(1)$ cm^{-1}, $g = 2.00(1)$; $J = -0.20(1)$, $g = 2.00(1)$ for **1** and **2** respectively, Fig. 5. The very low J values for **1** and **2** are in accordance with previously published MO calculations[10] which conclude that the $\mu_{1,5}$-dicyanamide bridge should be assumed to be a very poor superexchange mediator. EPR spectra recorded on powdered samples at room temperature show a broad isotropic signal centred at $g = 2.08$ (peak-to-peak linewidth 1108 G) for **1** and also a isotropic signal centred at $g = 2.03$ (peak-to-peak linewidth 423 G) for **2**.

Acknowledgements

This research was partially supported by Comisión Interministerial de Ciencia y Tecnologica (Grant PB96/0163) and OENB (grant 7967). F. A. Mautner thanks Professor C. Kratky and Dr Belaj (University of Graz) for use of experimental equipment.

References

1 S. R. Batten, P. Jensen, B. Moubaraki, K. S. Murray and R. Robson, *Chem. Commun.*, 1998, 439.
2 M. Kurmoo and C. J. Kepert, *New. J. Chem.*, 1998, 1515.
3 J. L. Manson, C. R. Kmety, Q. Huang, J. W. Lynn, G. M. Bendele, S. Pagola, P. W. Stephens, L. M. Liable-Sands, A. L. Rheingold, A. J. Epstein and J. S. Miller, *Chem. Mater.*, 1998, **10**, 2552.
4 J. L. Manson, C. R. Kmety, A. J. Epstein and J. S. Miller, *Inorg. Chem.*, 1999, **38**, 2552.
5 P. Jensen, S. R. Batten, G. D. Fallon, D. C. R. Hockless, B. Moubaraki, K. S. Murray and R. Robson, *J. Solid State Chem.*, 1999, **145**, 387.
6 J. L. Manson, D. W. Lee, A. L. Rheingold and J. S. Miller, *Inorg. Chem.*, 1998, **37**, 5966.
7 J. L. Manson, C. D. Incarvito, A. L. Rheingold and J. S. Miller, *J. Chem. Soc.*, *Dalton Trans.*, 1998, 3705.
8 S. R. Batten, P. Jensen, C. J. Kepert, M. Kurmoo, B. Moubaraki, K. S. Murray and D. J. Price, *J. Chem. Soc.*, *Dalton Trans.*, 1999, 2987.
9 J. L. Manson, A. M. Arif and J. S. Miller, *J. Mater. Chem.*, 1999, **9**, 979.
10 A. Escuer, F. A. Mautner, N. Sanz and R. Vicente, *Inorg. Chem.*, 2000, **39**, 1668.
11 J. L. Manson, A. M. Arif, C. D. Incarvito, L. M. Liable-Sands, A. L. Rheingold and J. S. Miller, *J. Solid State Chem.*, 1999, **145**, 369.
12 J. L. Manson, A. M. Arif and J. S. Miller, *Chem. Commun.*, 1999, 1479.
13 M. A. M. Abu-Youssef, A. Escuer, D. Gatteschi, M. A. S. Goher, F. A. Mautner and R. Vicente, *Inorg. Chem.*, 1999, **38**, 5716.
14 G. M. Sheldrick, SHELXS 86, Program for the Solution of Crystal Structure, University of Göttingen 1986.
15 G. M. Sheldrick, SHELXL 93, Program for the Refinement of Crystal Structure, University of Göttingen, 1993.
16 SHELXTL 5.03 (PC-Version), Program library for the Solution and Molecular Graphics, Siemens Analytical Instruments Division, Madison, WI, 1995.
17 A. L. Spek, PLUTON 92, University of Utrecht, 1992.
18 C. K. Johnson, ORTEP II, Report ORNL-5138, Oak Ridge National Laboratory, Oak Ridge, TN, 1976.
19 M. E. Fisher, *Am. J. Phys.*, 1964, **32**, 343.